Inverse Problems in Science and Engineering
Publication details, including instructions for authors and subscription information:
http://www.tandfonline.com/loi/gipe20

Modelling mechanical interfaces experiencing micro-slip/slap

H. Jalali [a], A. Hedayati [b] & H. Ahmadian [b]

[a] IUST-Arak Branch, Iran University of Science and Technology, Arak, Iran

[b] Center of Excellence in Solid Mechanics and Dynamics, Iran University of Science and Technology, Tehran, Iran

Available online: 06 Feb 2011

To cite this article: H. Jalali, A. Hedayati & H. Ahmadian (2011): Modelling mechanical interfaces experiencing micro-slip/slap, Inverse Problems in Science and Engineering, 19:6, 751-764

To link to this article: http://dx.doi.org/10.1080/17415977.2010.531467

Inverse Problems in Science and Engineering
Vol. 19, No. 6, September 2011, 751–764

Taylor & Francis
Taylor & Francis Group

Modelling mechanical interfaces experiencing micro-slip/slap

H. Jalali[a]*, A. Hedayati[b] and H. Ahmadian[b]

[a]*IUST-Arak Branch, Iran University of Science and Technology, Arak, Iran;* [b]*Center of Excellence in Solid Mechanics and Dynamics, Iran University of Science and Technology, Tehran, Iran*

(*Received 5 February 2010; final version received 6 October 2010*)

Surface-to-surface contact interfaces significantly affect structural behaviour. Therefore, accurate modelling of the stiffness and damping characteristics of such interfaces is crucial for dynamic response analysis of assembled structures. Due to the development of nonlinear interactions, such as slip and slap mechanisms, modelling and analysis of the contact interfaces is a challenging task. The nonlinear effects of the slip and slap mechanisms need to be considered in interface models particularly when the amplitude of the structural response is high. This article considers finite element (FE) modelling of a compound structure containing a surface-to-surface contact interface, i.e. a bolted lap-joint. The joint, modelled using thin-layer element theory, experiences micro-slips/slaps under extreme loading conditions of the structure and to take into account these behaviours, the thin-layer element is assumed to behave in a nonlinear manner. In order to identify the nonlinear uncertainties in the joint interface, the real structure is subjected to vibrational testing, and its dynamical behaviour at different loading levels is extracted. The parameters of interfacial elements are tuned in such a way that the resultant FE model predicts the experimental results with a high accuracy.

Keywords: nonlinear contact interface; thin-layer element; parameter identification

1. Introduction

Built-up structures are usually assembled using different types of joints and fasteners. Among these joints and fasteners are the bolted lap-joints. Bolted lap-joints, having surface-to-surface contact interfaces, impose nonlinearity in the dynamic response of the structures due to the nonlinear mechanisms developing at their interface area. Constructing accurate numerical representations of compound structures' dynamics demands precise models for contact interfaces. Such precise models can be achieved using experimental results. A group of elements usually used for modelling surface-to-surface contact interfaces are interface elements.

Interface elements have been found suitable for modelling contact interfaces since the idea was first pioneered by Goodman *et al.* [1] at 1968. There are two types of interface elements known as zero-thickness interface elements and thin-layer interface elements. The thickness of the contact interface is assumed zero in zero-thickness interface elements [2].

*Corresponding author. Email: jalali@iust.ac.ir

ISSN 1741–5977 print/ISSN 1741–5985 online

DOI: 10.1080/17415977.2010.531467
http://www.informaworld.com

Then, a constitutive law which usually consists of constant values for both the shear stiffness and the normal stiffness is defined for the element. In thin-layer interface elements, the behaviour of the contact interface is assumed to be controlled by a narrow band or zone adjacent to the interface with different properties from those of the surrounding materials [3,4]. The thin-layer element is treated as any other element of the finite element (FE) mesh and a special constitutive relation is assigned to it.

Interface elements first originated in geo-mechanics for modelling rock–rock contact problems. Since then, there have been many papers published on their applications; see, for example, Desai *et al*. [3], Sharma and Desai [5] and Pande and Sharma [6]. Thin-layer elements were also applied in structural model updating by Ahmadian *et al*. [7–9]. They showed that the thin-layer elements with a linear elastic constitutive relation can be used in model updating of contact stiffness coefficients using experimental data. Bograd *et al*. [10] used the thin-layer element concept for joint damping prediction. Mayer and Gaul [11] proposed a nonlinear thin-layer element and showed its capability in modelling the contact interface of bolted joints.

In this article, a 2D nonlinear thin-layer element is proposed which can be used for modelling the contact interface of a bolted lap-joint in an assembled structure. It is assumed that the behaviour of the thin-layer element in normal and tangential directions is independent. Using this assumption, the formulation of stiffness matrix is derived. A nonlinear thin-layer element is then presented by assuming that the parameters of the obtained thin-layer element are dependent upon the structural response. An experimental case study is considered and the linear parameters of the thin-layer element and their dependence on the response amplitude level are identified using experimental results.

2. Thin-layer element formulation

Figure 1 shows an assembly composed of two substructures connected through a contact interface. The contact interface, being provided by means of a compressive force P, transmits the forces between substructures. The compressive force P and the amplitude of the external applied forces are key factors in developing the mechanisms transmitting the forces at the contact interface. At high compressive forces or low excitation amplitudes, these mechanisms are linear. When the compressive force is decreased or the amplitude of the applied force is increased, nonlinear mechanisms contribute in transmitting the forces at the contact interface.

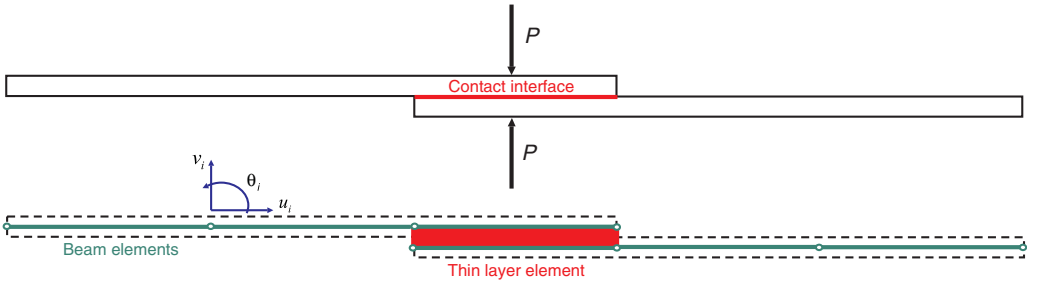

Figure 1. The structure including a contact interface and its corresponding FE model.

During modelling of the structures such as the one shown in Figure 1, we always encounter difficulties and complexities in describing the contact interface in mathematical representations, especially when the structural behaviour is nonlinear. In these conditions, operators governing the dynamics of the contact interface are hard to clarify [12]. In other words, when modelling of the structure shown in Figure 1 is considered, two substructures can be modelled easily using beam elements from FE theory (Figure 1). But modelling the interface area precisely is a challenging task. In fact, finding a suitable element (or operator) for modelling the contact interface needs more efforts compared to modelling the beam sections of the structure. In this article, a nonlinear thin-layer element is considered to represent the dynamics of the contact interface. Although this article considers modelling the contact interfaces in beam structures, the idea is general and can be easily extended to other cases.

A schematic of an assembly consisting of two beam substructures is shown in Figure 1. The beam sections of the structure are modelled using 2D Euler–Bernoulli beam elements [13], each having three degrees-of-freedom (DOF) per node. The DOF of the beam elements are considered as $d_i = [u_i, v_i, \theta_i]^{\mathrm{T}}$; where u_i and v_i are, respectively, the displacements in longitudinal and lateral directions and θ_i is the rotation about the axis perpendicular to the element plane. A 2D thin-layer element is used for modelling the joint interface. Figure 1 also shows a schematic of the FE model of the structure.

For consistency's sake, the thin-layer element used for modelling the contact interface is assumed to have the same DOF per node as the beam elements do. Figure 2 shows a typical 2D thin-layer element. The elements' dimensions are considered as: l (length), h (height) and t (thickness).

The beam elements are located on the neutral axis of the beam sections of the structure. Therefore the height, i.e. h, of the thin-layer element is obtained equal to the thickness of the beam sections. The thickness of the thin-layer element, i.e. t, is considered equal to the width of the beam sections. In order to calculate the stiffness matrix of the element shown in Figure 2, which is a 2D plane element, a constitutive relation needs to be defined. Equation (1) shows the assumed constitutive relation for this element [3–5].

$$\begin{Bmatrix} \sigma_y \\ \tau_{xy} \end{Bmatrix} = \begin{bmatrix} E' & 0 \\ 0 & G' \end{bmatrix} \begin{Bmatrix} \varepsilon_y \\ \gamma_{xy} \end{Bmatrix}, \quad \text{or } \{\boldsymbol{\sigma}\} = [\mathbf{D}']\{\boldsymbol{\varepsilon}\}, \tag{1}$$

where $\varepsilon_y = \frac{\partial v}{\partial y}$ and $\gamma_{xy} = \frac{1}{2}\left(\frac{\partial u}{\partial y} + \frac{\partial v}{\partial x}\right)$.

In Equation (1), E' and G' correspond to the normal and shear stiffness coefficients of the contact interface, respectively. Since the movement in the normal/tangential direction does not invoke any contraction in tangential/normal direction, the normal contact behaviour is decoupled from the shear contact behaviour. Therefore, in Equation (1), the off-diagonal terms are equated to zero. In the theory of thin-layer element proposed by Desai *et al.* [3], it is assumed that the contact interface has stiffness in normal (i.e. y) and shear (i.e. xy) directions; the stiffness in the x direction is considered negligible.

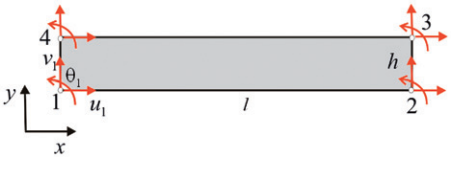

Figure 2. The 2D thin-layer element.

Having the stress–strain constitutive relation known in Equation (1), one may obtain the stiffness matrix of the thin-layer element as

$$[\mathbf{K}'] = t\int_0^h \int_0^l [\mathbf{B} \quad \mathbf{Q}]^T[\mathbf{D}'][\mathbf{B} \quad \mathbf{Q}]\mathrm{d}x\,\mathrm{d}y, \tag{2}$$

where [**B**] and [**Q**] are matrices mapping the strain vector to the displacement and the rotation fields of the element, respectively. The displacement and the rotation fields are related to the element nodal DOF vector through the shape functions. For more details about the shape functions and matrices [**B**] and [**Q**] for the element shown in Figure 2, see [14]. The normal and shear stiffness coefficients of the contact interface, i.e., E' and G', can be identified using experimental results. This issue will be covered in detail in the following sections. Equation (2) offers the stiffness matrix of a linear thin-layer element. In the following paragraphs a nonlinear thin-layer element useful for modelling nonlinear contact interfaces is presented.

Under low excitation amplitudes – and provided that the pre-load P (Figure 1) is high enough to prevent nonlinear interactions – the behaviour of the contact interface is linear. In such circumstances, the parameters of the above introduced thin-layer element are constant. Identification of the linear/constant interface models/parameters has been the subject of many papers in the past [9,15,16]. Nonlinear mechanisms develop at the contact interface when excitation amplitude is high enough to initiate them. Accurate modelling of the nonlinear interface needs precise nonlinear models. These models can be obtained using experimental observations. Previous experimental investigations show that the interface behaviour is dependent upon the amplitude of the structural response [12,17,18]. This indicates the presence of nonlinearity in the contact interface. The effects of this nonlinearity can be taking into account by employing nonlinear interface models in mathematical representations of the structure. A set of nonlinear interface elements can be obtained by employing nonlinear stress–strain constitutive relations in Equation (1). For example, Mayer and Gaul [11] used a piecewise linear elastic penalty law for modelling normal behaviour and a Masing-element for modelling tangential behaviour of the contact interface and obtained a nonlinear thin-layer element. Equation (3) shows the constitutive law they used for normal contact

$$p_y = -\sigma_y = \begin{cases} 0, & \text{for } \Delta v > g_0, \\ c_1(g_0 - \Delta v), & \text{for } g_0 \geq \Delta v > 0, \\ c_1 g_0 - c_2 \Delta v, & \text{for } 0 \geq \Delta v > -g_0, \\ (c_1 + c_2) g_0 - c_3(\Delta v + g_0), & \text{for } \Delta v \leq -g_0, \\ & c_3 < c_2 < c_1 < 0, \end{cases} \tag{3}$$

where Δv is the relative normal distance (gap) between the two bodies, and g_0 is a reference gap distance at which a contact pressure p_y starts to be transmitted between the bodies.

Stress–strain relationships like the one shown in Equation (3) are more suitable when modelling and analysis of the contact interfaces in time domain are considered. In frequency domain analysis, a different strategy as described following may be adopted.

Assuming that a general nonlinear function as in Equation (4) governs the stress–strain relationship

$$\sigma(t) = f(\varepsilon(t), \dot{\varepsilon}(t)). \tag{4}$$

Also considering that the excitation force is mono-harmonic, the structural response and consequently the strain can be assumed mono-harmonic too, i.e. $\varepsilon(t) = Y_\varepsilon \sin(\omega t + \theta)$. Using the describing function concept [19], a linearized stress–strain relationship can be obtained as

$$\sigma(t) \cong (\mathrm{E}_r(Y_\varepsilon, \omega) + j\mathrm{E}_i(Y_\varepsilon, \omega))\varepsilon(t) = \mathrm{E}_{eq}(Y_\varepsilon, \omega)\varepsilon(t), \tag{5}$$

where

$$\mathrm{E}_{\mathrm{eq}}(Y_\varepsilon, \omega) = \frac{1}{\pi Y_\varepsilon}\int_0^{2\pi} f(Y_\varepsilon \sin(\tau), \omega Y_\varepsilon \cos(\tau))(\sin(\tau) + j\cos(\tau))\mathrm{d}\tau, \quad \tau = \omega t + \theta. \tag{6}$$

Equation (5) shows that in the case of analysis in the frequency domain a displacement dependent stress–strain relationship can be used in Equation (1). Following the above discussion, a nonlinear thin-layer element is proposed in this article for modelling nonlinear contact interfaces by considering that the parameters of the thin-layer element introduced in Equation (1) are the functions of structural response amplitude level. In general, if K' is a nonlinear interface parameter, it is considered to be of the following form:

$$K' = K'_0 + g(X), \tag{7}$$

where K'_0 is the linear interface parameter and X is the structural response amplitude level to harmonic excitation force. X is a measurable quantity and has a direct relationship to the dynamic strain amplitude in the contact interface (Y_ε in Equation (5)). In the following applications, ω – the excitation frequency – changes in a small interval, usually in a 1.5 Hz frequency interval, therefore the dependence of the interface parameters to ω is negligible; hence, it was omitted from Equation (7).

$g(X)$ is a nonlinear complex function where its real and imaginary parts, respectively, models the stiffness and damping nonlinearity at the contact interface. In the case of modelling of the stiffness, $g(X)$ is a negative-valued function ensuring that the stiffness characteristic of the contact interface decreases as response amplitude level is increased – the well-known softening-effect phenomena. While in the case of modelling the damping characteristics, $g(X)$ is a positive-valued, monotonically increasing function indicating that the damping characteristic of the contact interface increases as response amplitude level is increased – i.e. contact interfaces such as joints have shown to experience hardening damping characteristics [12,18].

It is worth mentioning that the stress–strain relationship used in this article for modelling the nonlinear behaviour of the contact interface, i.e. Equation (5), is considered to be a function of response amplitude level. This means that a hyperelastic material model is used for representing the behaviour of the contact interface. Hyperelasticity is a collective term for a family of models that have a strain energy density that depends only upon the currently applied deformation state (and not on the history of deformation). This class of material models is characterized by a nonlinear elastic response and does not capture yielding [20].

The linear stiffness parameters of the contact interface are identified in this article by using linear natural frequencies and adopting an eigenvalue sensitivity approach. The parameters of the nonlinear function $g(X)$ are then estimated using experimental nonlinear frequency response functions (FRFs) and employing an FRF-based sensitivity approach. In the following section, an experimental case study is described.

3. Experimental case study

The experimental bolted joint coupling two identical steel beams is shown in Figure 3. The beam has the following parameters: $L = 420$ mm (overall length), $b = 25.4$ mm (width) and $h = 6.36$ mm (thickness). The fixed-free boundary condition is chosen which makes excitation of nonlinear mechanisms at the contact interface easier. The structure is excited using a concentrated external force applied by means of an electromagnetic shaker through a stinger at position $x = 50$ mm. The excitation point is chosen to be close to the fixed end of the structure in order to minimize any unwanted nonlinearities arising in the magnetic field of the shaker. A force transducer is used between shaker and structure in order to measure the applied force. The structural response is measured by means of two accelerometers in positions $x = 300$ mm and $x = 420$ mm. The force cell placed under the bolt head makes measurement of the bolt pre-load possible.

The experiments are completed for two different bolt pre-loads, i.e. 120 and 540 N. At each pre-load, three different excitation levels are used, $F = 1.5$, $F = 3.0$ and $F = 6$ N. First, the structure is excited using a low-level random excitation signal and linear FRFs are measured. The experimental FRFs are shown in Figure 4 and corresponding natural frequencies are tabulated in Table 1. The linear natural frequencies are used in the following section and a linear FE model of the structure is constructed.

In the second stage of experiments, the structure is excited using a harmonic force and the excitation frequency is varied slowly in a band of 1.5 Hz around the first natural frequency. The excitation amplitude is maintained at a constant level for all excitation frequencies and the steady-state response of the structure and its corresponding force signal are recorded. The nonlinear FRFs are constructed using the measured response and excitation signals. The FRFs are shown in Figure 5 and correspond to the accelerometer closest to the tip of the beam.

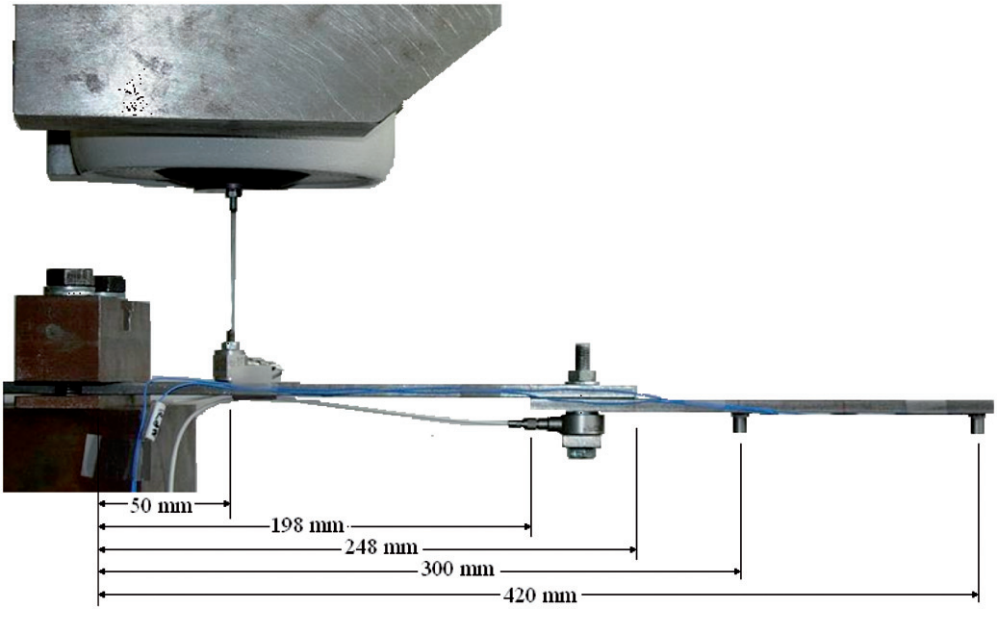

Figure 3. Test structure with an interface area of $50 \times 25.4\,\text{mm}^2$, structure geometrical dimensions and the location of applied force and measurements.

Shifting of the resonant points to lower frequencies and decreasing of the peak amplitudes when excitation force amplitude is increased indicate the presence of nonlinearity in contact interface. Also, the jump phenomenon which is a sign of nonlinearity is evident from the FRFs shown in Figure 5. By jump phenomena it means the sudden increase in response amplitude due to a small increase in excitation frequency. The following section considers identification of the thin-layer element parameters using experimental results presented in this section.

4. Identification of thin-layer element linear parameters

4.1. *FE modelling*

The FE model of the structure shown in Figure 3 is constructed using 41 2D Euler–Bernoulli beam elements [13] for modelling two beam sections and three 2D thin-layer elements for modelling the contact interface. The material properties of the beam sections

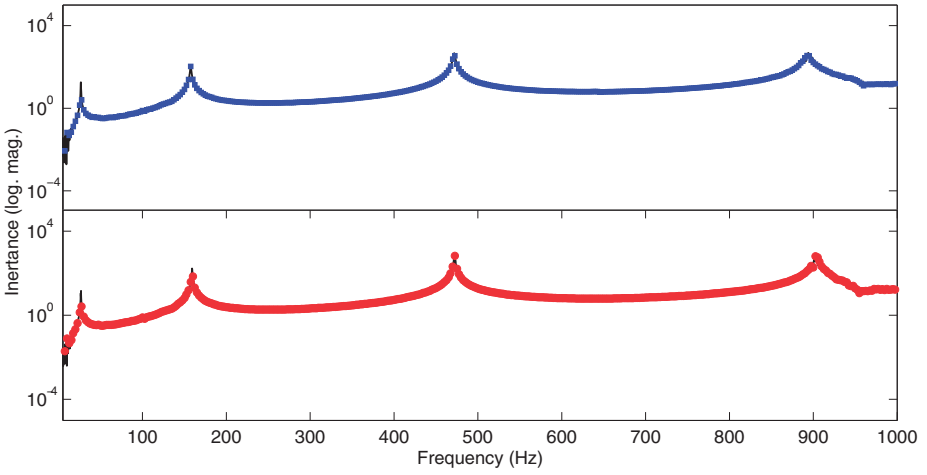

Figure 4. Linear FRFs: pre-loads of 120 N (■) and 540 N (●).

Table 1. Experimental and updated natural frequencies at different pre-loads.

	Pre-load: 120 N $E_0' = 3.9 \times 10^8\,\mathrm{N\,m^{-2}}$, $G_0' = 7.6 \times 10^7\,\mathrm{N\,m^{-2}}$			
	ω_1 (Hz)	ω_2 (Hz)	Ω_3 (Hz)	ω_4 (Hz)
Experimental	26.50	157.60	471.80	895.00
Updated	26.53	157.82	477.24	891.69
Error (%)	−0.11	−0.14	−0.15	0.36
	Pre-load: 540 N $E_0' = 5.9 \times 10^8\,\mathrm{N\,m^{-2}}$, $G_0' = 7.4 \times 10^7\,\mathrm{N\,m^{-2}}$			
Experimental	26.60	159.20	472.50	904.00
Updated	26.54	159.15	477.59	900.23
Error (%)	0.18	0.02	−1.07	0.41

are: $\rho = 7880\,\mathrm{kg\,m^{-3}}$ and $E = 198\,\mathrm{GPa}$. The parameters of three thin-layer elements are assumed to be the same. The stiffness effect of the bolt and also mass effects of the bolt, force cell, force transducer and accelerometers are also included in the FE model. The FE model is updated and the linear parameters of the thin-layer element are identified using linear natural frequencies.

4.2. *Identification of linear thin-layer element parameters*

First, formulation of the linear thin-layer element (Equation (1)) is used and an FE model for linear behaviour of the structure is constructed. A schematic of the FE mesh is shown in Figure 6. The linear parameters of the stiffness matrix of the thin-layer elements, i.e. E_0' and G_0', are identified at different pre-loads using linear natural frequencies presented in Table 1. For this end, an objective function of the form $\sum W_i(\omega_{ie}^2 - \omega_{ia}^2)$ is minimized using

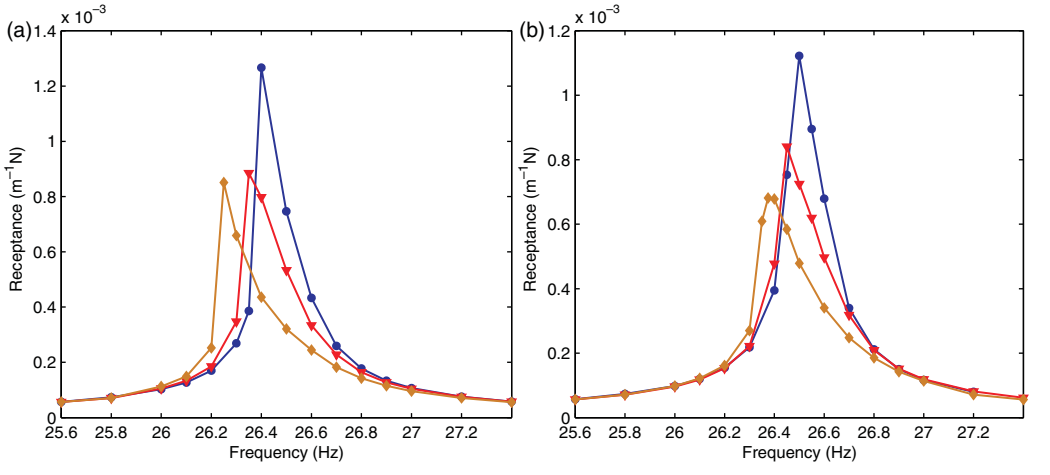

Figure 5. Nonlinear FRFs at different excitation levels: $F = 1.5\,\mathrm{N}$ (●), $F = 3\,\mathrm{N}$ (▼) and $F = 6\,\mathrm{N}$ (◆); pre-loads of 540 N (right) and 120 N (left).

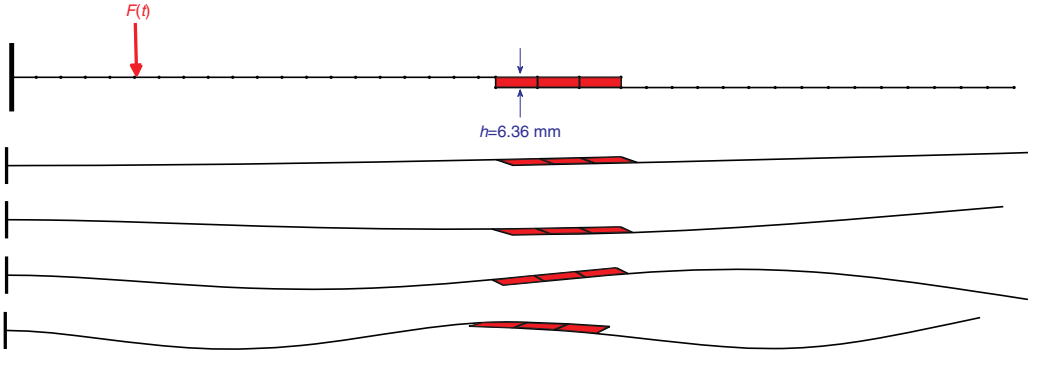

Figure 6. FE mesh and the mode shapes of the updated FE model.

the eigensensitivity updating approach and adjusting the linear parameters of the stiffness matrix; ω_{ie} and ω_{ia} are, respectively, the experimental and numerical natural frequencies and W_i is a weighting factor. The initial values for linear parameters, for example at pre-load of 120 N, are selected as $E'_{0-i} = 3 \times 10^9\,\mathrm{N\,m^{-2}}$ and $G'_{0-i} = 5.2 \times 10^6\,\mathrm{N\,m^{-2}}$. After performing minimization, these parameters are updated to $E'_{0-u} = 3.9 \times 10^8\,\mathrm{N\,m^{-2}}$ and $G'_{0-u} = 7.6 \times 10^7\,\mathrm{N\,m^{-2}}$. Table 1 shows the experimental and updated natural frequencies and their differences. Also, the updated linear parameters of the contact interface at different pre-loads are presented in Table 1.

Results shown in Table 1 indicate that the linear thin-layer element is capable of modelling the joint interface with an acceptable accuracy. In Figure 6, the mode shapes of the updated FE model at pre-load of 540 N are presented.

The mode shapes shown in Figure 6 are consistent with the experimental mode shapes of the structure, which are more or less similar to the mode shapes of a clamped beam. Also from Figure 6, it is obvious that the contact elements undergo shear and normal deformations, especially in modes 1, 2 and 4. Shear and normal deformations, respectively, resemble micro-slip and micro-slap mechanism at the contact interface. In the previous section, the experimental results for high excitation amplitudes – i.e. higher than those used in measuring the linear FRFs – are presented. At high excitation amplitudes the above-mentioned nonlinear mechanisms develop at the contact interface. In the following, identification of the nonlinear parameters of these mechanisms is considered.

5. Identification of thin-layer element nonlinear parameters

5.1. *Nonlinear thin-layer element formulation*

The nonlinear formulation of the thin-layer element is used and a nonlinear FE model of the structure is constructed. As stated in Equation (7), in nonlinear thin-layer elements, the interface parameters are functions of response amplitude level. A sensitivity analysis shows that the nonlinear response of the structure near its first resonant frequency is mostly dominated by the stiffness of the contact interface in normal direction and the damping of the contact interface in tangential direction. Therefore, in order to find a joint model capable of representing the nonlinear dynamics of the contact interface, the parameters of the nonlinear thin-layer element are assumed to have the following forms:

$$E'(X) = E'_0 - g_1(X), \tag{8}$$

$$G'(X) = G'_0 + jg_2(X), \tag{9}$$

where X is the measured response amplitude level of the structure at different excitation frequencies. E'_0 and G'_0 are the linear parameters of the linear thin-layer element identified in the previous section using linear natural frequencies (Table 1). $g_1(X)$ and $g_2(X)$ are nonlinear functions representing the nonlinearity in stiffness and damping characteristics of the contact interface. A polynomial form as the following one is considered for these functions:

$$g_i(X) = \alpha_{i1} + \alpha_{i2}X + \alpha_{i3}X^2 + \cdots, \quad i = 1, 2. \tag{10}$$

α_{ij} will be identified later in this section using experimental frequency response curves shown in Figure 7. By substituting Equations (8)–(10) into Equation (1), the stiffness

matrix for the nonlinear thin-layer elements is obtained, which is composed of linear and nonlinear parts as described as

$$\mathbf{K}' = \mathbf{K}'_{\mathbf{L}}(E'_0, G'_0) + \left(\mathbf{K}'_{\mathbf{NL-r}}(X) + j\mathbf{K}'_{\mathbf{NL-i}}(X)\right). \tag{11}$$

Having the stiffness matrix of the thin-layer elements known in Equation (11) and by using the mass and stiffness matrices of the Euler–Bernoulli beam elements [13] for modelling beam sections, an FE model is constructed for predicting the dynamic properties of the structure. The equation of motion of the FE model is shown as

$$[\mathbf{M}]\{\ddot{x}\} + ([\mathbf{K}] + [\mathbf{K_{NL-r}}] + j[\mathbf{K_{NL-i}}])\{x\} = \{f\}, \tag{12}$$

where real and imaginary parts of $[\mathbf{K_{NL}}]$ contain unknown parameters α_{ij} which need to be identified. A frequency response sensitivity-based identification approach is used for identification of these parameters.

5.2. *FRF sensitivity method and parameter regularization*

The nonlinear stiffness matrix in Equation (12) depends upon the structural response amplitude X. In the case of exciting the structure using sinusoidal forces, similar to what was described in experimental section, the structural response in steady-state condition has constant amplitude and hence X is constant. Therefore, the global stiffness matrix is constant in a specific excitation frequency. Under these circumstances, one may obtain the frequency response matrix by assuming a harmonic response for the structure and substituting it into Equation (12). This finally results in

$$[\mathbf{H}(\omega_k)] = \left((\mathbf{K} + \mathbf{K_{NL-r}} + j\mathbf{K_{NL-i}}) - \omega_k^2\mathbf{M}\right)^{-1}. \tag{13}$$

The sensitivity of frequency response matrix, $[\mathbf{H}(\omega_k)]$, with respect to an updating parameter, φ, can be obtained as [21]

$$\frac{\partial[\mathbf{H}(\omega_k)]}{\partial\varphi} = -[\mathbf{H}(\omega_k)]\frac{\partial[\mathbf{Z}(\omega_k)]}{\partial\varphi}[\mathbf{H}(\omega_k)], \quad \text{where } [\mathbf{Z}(\omega_k)] = [\mathbf{H}(\omega_k)]^{-1}. \tag{14}$$

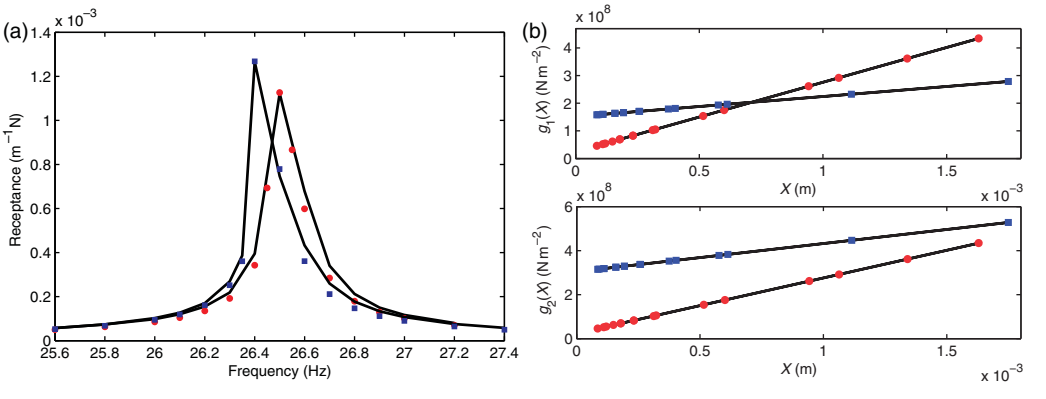

Figure 7. Experimental (lines) and predicted (marks) FRFs (left), updated functions g_1(X) and g_2(X) (right); at pre-loads of 120 N (■) and 540 N (●).

By substituting Equation (13) into Equation (14) and assuming that response and excitation coordinates are nodes i and j, respectively, the sensitivity of $H_{ij}(\omega_k)$ with respect to φ can be expressed as

$$\frac{\partial H_{ij}(\omega_k)}{\partial \varphi} = -\left\{H_i^a(\omega_k)\right\}^{\mathrm{T}} \frac{\partial \mathbf{Z}(\omega_k)}{\partial \varphi} \left\{H_j^a(\omega_k)\right\}, \tag{15}$$

where $\{H_i^a(\omega)\}^{\mathrm{T}}$ and $\{H_j^a(\omega)\}$ are ith row and jth column vectors of analytical frequency response matrix. In this article, logarithmic frequency response sensitivity (in dB scale) is used [22].

$$\frac{\partial\left(20\log_{10}\left|H_{ij}(\omega_k)\right|\right)}{\partial \varphi} = \frac{20}{\log_e 10}\left(\frac{\Re\left(H_{ij}(\omega_k)\right)\frac{\partial \Re\left(H_{ij}(\omega_k)\right)}{\partial \varphi} + \Im\left(H_{ij}(\omega_k)\right)\frac{\partial \Im\left(H_{ij}(\omega_k)\right)}{\partial \varphi}}{\Re\left(H_{ij}(\omega_k)\right)^2 + \Im\left(H_{ij}(\omega_k)\right)^2}\right). \tag{16}$$

By using Equation (16) in every excitation frequency, the updating problem can be simplified in a matrix form as $[\mathbf{S}]\{\Delta\varphi\} = \{\varepsilon\}$. Here, $[\mathbf{S}]$ is the sensitivity matrix, $\{\Delta\varphi\}$ is the updating parameter vector and $\{\varepsilon\}$ is the output residual vector composing the differences between experimental and numerical frequency responses. For the problem considered in this article, $\{\Delta\varphi\}$ is $[\Delta\alpha_{11}, \Delta\alpha_{12}, \Delta\alpha_{13}, \ldots, \Delta\alpha_{21}, \Delta\alpha_{22}, \Delta\alpha_{23}, \ldots]^{\mathrm{T}}$. Note that updating requires an iterative process due to the first-order approximation of sensitivity with respect to an updating parameter. A problem encountered in the FRF model updating is ill-conditioning of the sensitivity matrix $[\mathbf{S}]$. Ill-conditioned sensitivity matrices may lead to numerical instability in the solution process. Also, in ill-posed problems the existence and uniqueness of a solution is not assured [23,24]. In this article, a Tikhonov regularization technique is used [25] in order to overcome the ill-conditioning of the sensitivity matrix. In the Tikhonov regularization technique, the updating problem $[\mathbf{S}]\{\Delta\varphi\} = \{\varepsilon\}$ at kth iteration is redefined as minimization of the following objective function:

$$\mathbf{J}_{\Delta\varphi} = \left\|[\mathbf{S}]\{\Delta\varphi\} - \{\varepsilon\}\right\|_2^2 + \lambda^2\left\|\{\Delta\varphi\}\right\|_2^2, \tag{17}$$

where λ is the regularization parameter. Two methods, i.e. the L-curve method and generalized cross-validation, have been proposed for selection of the regularization parameter in the Tikhonov regularization technique [26]. In this article, the method described in [27] which is based on the L-curve method is used in updating iterations for finding λ.

In the following sections, the results obtained using the FRFs shown in Figure 5, in Equation (16) and the identified parameters are presented.

5.3. *Nonlinear thin-layer element identification results*

First, identification of the nonlinear interface parameters in excitation amplitude of 1.5 N is considered. Linear functions are considered for $g_1(X)$ and $g_2(X)$ at two different pre-loads, i.e., 120 and 540 N. By following the above-described identification procedure, the parameters of functions $g_1(X)$ and $g_2(X)$ are updated iteratively until convergence is achieved. In Figure 7, the experimental FRFs are compared with the FRFs obtained using the updated thin-layer element. On the right-hand side of Figure 7, updated $g_1(X)$ and $g_2(X)$ are depicted as functions of the measured response amplitude level.

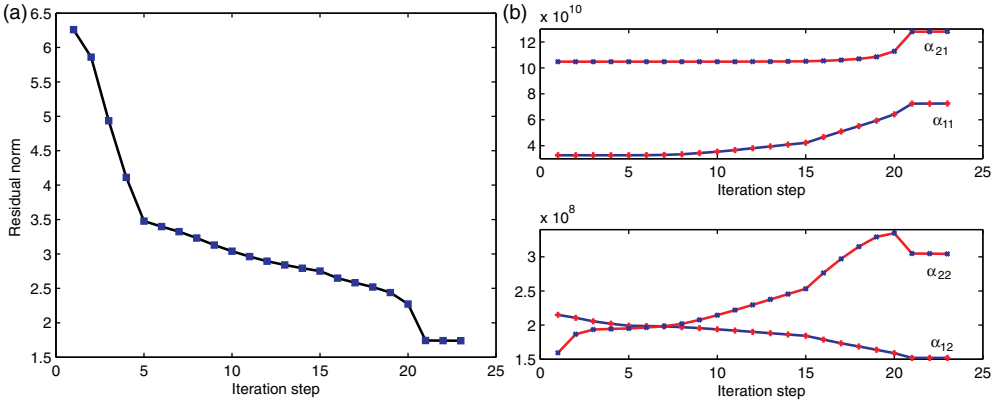

Figure 8. Changes in objective function (left) and updating parameters (right) at a pre-load of 120 N.

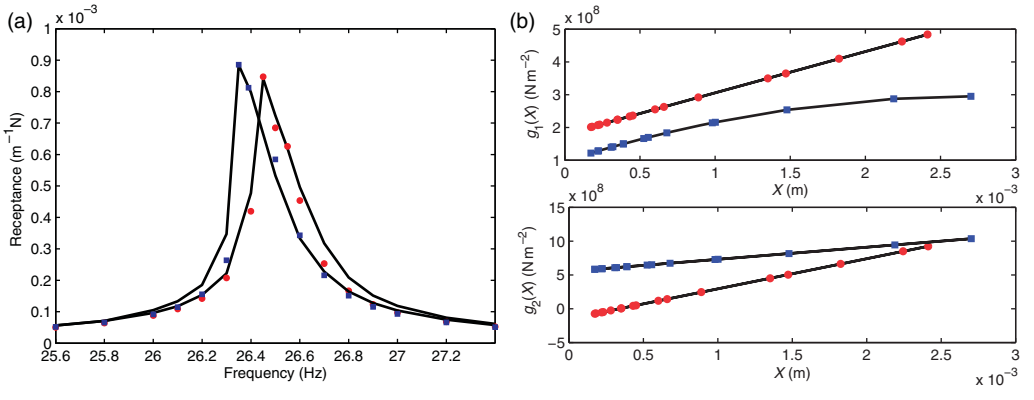

Figure 9. Experimental (lines) and predicted (marks) FRFs (left), updated functions g_1(X) and g_2(X) (right); pre-loads of 120 N (■) and 540 N (●).

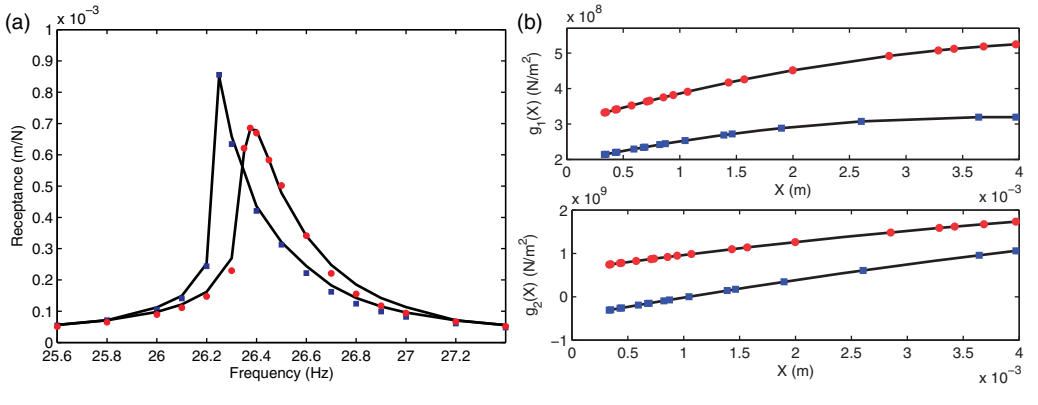

Figure 10. Experimental (lines) and predicted (marks) FRFs (left), updated functions g_1(X) and g_2(X) (right); pre-loads of 120 N (■) and 540 N (●).

The changes in objective function and updating parameters are shown in Figure 8 and correspond to the pre-load of 120 N. This figure shows that after 23 iterations, the objective function converges to the measured target values. Within these optimization iterations, the reduction of objective function is about 72% and updating parameters experience changes between 22% (α_{21}) and 122% (α_{11}).

Next, identification of the nonlinear thin-layer element parameters at an excitation amplitude of 3 N is considered. In this excitation amplitude, linear functions are considered for $g_1(X)$ and $g_2(X)$ at pre-load of 540 N. For pre-load of 120 N, $g_1(X)$ is found to be quadratic but again a linear function is obtained for $g_2(X)$. In Figure 9, experimental and predicted FRFs are shown. This figure also shows $g_1(X)$ and $g_2(X)$.

Finally, the measured nonlinear FRFs at an excitation amplitude of 6 N are used and the parameters of nonlinear thin-layer element are identified. At this excitation amplitude, quadratic functions are considered for $g_1(X)$ and $g_2(X)$ at two pre-loads, i.e. 120 and 540 N. Figure 10 shows the experimental and predicted FRFs.

The results shown in Figures 8–10 indicate that by increasing the excitation amplitude or decreasing the pre-load the order of the polynomials representing the nonlinearity in stiffness and damping characteristics of nonlinear thin-layer element increases. Also, comparison of the experimental FRFs and the FRFs obtained by updated models shows that the nonlinear thin-layer element is capable of representing the nonlinear mechanisms at the contact interface with an acceptable accuracy.

6. Conclusions

In this article, a nonlinear thin-layer element was introduced for modelling contact interfaces. The formulation of the stiffness matrix was derived and in order to take into account the nonlinear mechanisms developing at contact interface, its parameters were considered to be dependent upon the amplitude of the structural response. Experiments were conducted on a structure in two stages and its linear and nonlinear modal characteristics were measured. Using the linear experimental natural frequencies and by adopting an eigensensitivity approach, linear parameters of the thin-layer element were updated. The nonlinear parameters of contact interface were identified using nonlinear FRFs and by employing an FRF-based sensitivity approach. The results obtained from the identified model showed that the introduced contact interface model was able to simulate the experimental results with an acceptable accuracy.

References

[1] R.E. Goodman, R.L. Taylor, and T.L. Brekke, *A model for the mechanics of jointed rock*, J. Soil Mech. Found. Div. 59 (1968), pp. 99–637.

[2] G. Beer, *An isoparametric joint interface element for finite element analysis*, Int. J. Numer. Methods Eng. 21 (1985), pp. 585–600.

[3] C.S. Desai, M.M. Zaman, J.G. Lightner, and H.J. Siriwardane, *Thin-layer element for interfaces and joints*, Int. J. Numer. Anal. Meth. Geomech. 8 (1984), pp. 19–43.

[4] T.D. Lau, B. Noruziaan, and A.G. Razaqpour, *Modeling of construction joints and shear sliding effects on earthquake response of arch dams*, Earthquake Eng. Struct. Dyn. 27 (1998), pp. 1013–1029.

[5] K.G. Sharma and C.S. Desai, *Analysis and implementation of thin-layer element for interfaces and joints*, J. Eng. Mech. 118 (1992), pp. 2442–2462.
[6] G.N. Pande and K.G. Sharma, *On joint/interface elements and associated problems of ill-conditioning, short communications*, Int. J. Numer. Anal. Methods Geomech. 3 (1979), pp. 293–300.
[7] H. Ahmadian, M. Ebrahimi, J.E. Mottershead, and M.I. Friswell, *Identification of Bolted-joint Interface Models*, International Conference on Noise and Vibration Engineering (ISMA), Katholieke University, Leuven, Belgium, 2002.
[8] H. Ahmadian, H. Jalali, J.E. Mottershead, and M.I. Friswell, *Dynamic Modelling of Spot Welds using Thin-layer Interface Theory*, 10th International Congress on Sound and Vibration (ICSV 10), Stockholm, Sweden, 2003.
[9] H. Ahmadian, J.E. Mottershead, S. James, M.I. Friswell, and C.A. Reece, *Modeling and updating of large surface-to-surface joints in the AWE-MACE structure*, Mech. Syst. Sig. Process. 20 (2006), pp. 868–880.
[10] S. Bograd, A. Schmidt, and L. Gaul, *Joint Damping Prediction by Thin-layer Elements*, Proceedings of IMAC XXVI: A Conference and Exposition on Structural Dynamics, Orlando, FL, 2008.
[11] M.H. Mayer and L. Gaul, *Segment-to-segment contact elements for modeling joint interfaces in finite element analysis*, Mech. Syst. Sig. Process. 21 (2007), pp. 724–734.
[12] H. Jalali, H. Ahmadian, and J.E. Mottershead, *Identification of nonlinear bolted lap-joint parameters by force-state mapping*, Int. J. Sol. Struct. 44 (2007), pp. 8087–8105.
[13] J.N. Reddy, *An Introduction to the Finite Element Method*, McGraw-Hill, New York, 1984.
[14] A. Ibrahimbegovic, R.L. Taylor, and E.L. Wilson, *A robust quadrilateral membrane finite element with drilling degrees of freedom*, Int. J. Numer. Methods Eng. 30 (1990), pp. 445–457.
[15] Y. Ren and C.F. Beards, *Identification of effective linear joints using coupling and joint identification techniques*, ASME J. Vibr. Acoust. 120 (1998), pp. 331–338.
[16] W.L. Li, *A new method for structural model updating and joint stiffness identification*, Mech. Syst. Sig. Process. 16 (2002), pp. 155–167.
[17] H. Ahmadian and A. Zamani, *Identification of nonlinear boundary effects using nonlinear normal modes*, Mech. Syst. Sig. Process. 23 (2009), pp. 2008–2018.
[18] C.J. Hartwigsen, Y. Song, D.M. McFarland, L.A. Bergman, and A.F. Vakakis, *Experimental study of non-linear effects in a typical shear lap joint configuration*, J. Sound Vib. 277 (2004), pp. 327–351.
[19] A. Gelb and W.E. Vander Velde, *Multiple-input Describing Functions and Nonlinear System Design*, McGraw-Hill Book Co., New York, 1968.
[20] R.W. Ogden, *Large deformation isotropic elasticity: On the correlation of theory and experiment for incompressible rubber-like solids*, Proc. Roy. Soc. Lond. Ser. A 326 (1972), pp. 565–584.
[21] M.I. Friswell and J.E. Mottershead, *Finite Element Model Updating in Structural Dynamics*, Kluwer Academic, Dordrecht, 1995.
[22] H. Grafe, *Model updating of large structural dynamic models using measured response functions*, Ph.D. diss., Imperial College of Science Technology and Medicine, 1998.
[23] H.G. Natke, *On regularization method within system identification*, in Inverse Problems in Engineering Mechanics: IUTAM Symposium, M. Tanaka and H.D. Bui, eds., Springer, Berlin, 1993, pp. 3–20.
[24] A.N. Tikhonov, *Numerical Methods for the Solution of Ill-posed Problems*, Kluwer Academic Publishers, Boston, 1995.
[25] A.N. Tikhonov and V.Y. Arsenin, *Solutions of Ill-posed Problems*, John Wiley, New York, 1977.
[26] H. Ahmadian, J.E. Mottershead, and M.I. Friswell, *Regularization method for finite element model updating*, Mech. Syst. Sig. Process. 12 (1998), pp. 47–64.
[27] X.G. Hua, Y.Q. Ni, and J.M. Ko, *Adaptive regularization parameter optimization in output-error-based finite element model updating*, Mech. Syst. Sig. Process. 23 (2009), pp. 563–579.